

Density functional theory calculations on magnetic properties of actinide compounds

Denis Gryaznov,^{*ab} Eugene Heifets^a and David Sedmidubsky^c

Received 27th April 2010, Accepted 13th July 2010

DOI: 10.1039/c0cp00372g

We have performed a detailed analysis of the magnetic (collinear and non-collinear) order and the atomic and electron structures of UO_2 , PuO_2 and UN on the basis of density functional theory with the Hubbard electron correlation correction (DFT + U). We have shown that the 3-k magnetic structure of UO_2 is the lowest in energy for the Hubbard parameter value of $U = 4.6$ eV (and $J = 0.5$ eV) consistent with experiments when Dudarev's formalism is used. In contrast to UO_2 , UN and PuO_2 show no trend for a distortion towards rhombohedral structure and, thus, no complex 3-k magnetic structure is to be anticipated in these materials.

1. Introduction

Actinide compounds continue to attract a great interest for both materials scientists and nuclear engineers. Their properties combine a strong electron correlation and relativistic effects of 5f valence electrons. In this paper, we study collinear and non-collinear magnetic structures of three basic actinide materials UO_2 , PuO_2 and UN. All these materials have face-centred cubic (f.c.c.) actinide sub-lattice: the two oxides have fluorite structure and UN rock-salt structure. Experiments suggest that at low temperatures UN is anti-ferromagnetic¹ with a collinear magnetic order, where U magnetic moments alternate along the $\langle 001 \rangle$ direction, while UO_2 is anti-ferromagnetic (AFM) with the so-called noncollinear 3-k ordering of U magnetic moments (see Section 3 for more detailed description of different magnetic structures). The U magnetic moments in UN and UO_2 in the AFM phases are very different, being $0.75 \mu_B$ and $1.74 \mu_B$, respectively. The Néel temperatures for both UO_2 ($T_N = 30.8$ K, ref. 2) and UN ($T_N = 53$ K, ref. 1) are quite low. These two materials also differ in the chemical bonding. UN is evidently a conductor,³ whereas UO_2 is a Mott insulator (as discussed, for example, in ref. 4). PuO_2 is also a Mott insulator⁴ with magnetic susceptibility being temperature independent.⁵ All recent theoretical considerations^{6–9} employing the DFT + U technique or hybrid exchange–correlation functional (though without including spin–orbital interactions (SOI)) suggested the 1-k (collinear) AFM order for insulating PuO_2 , while experiment suggests that PuO_2 is diamagnetic.

Thus, it is important to compare magnetic orders and accompanying lattice distortions for three considered compounds (UO_2 , UN, and PuO_2) using the same method. Ignoring the lattice distortions may lead to a wrong electronic structure and significant errors in the defect energetics.¹⁰ As it was already mentioned, these materials reveal the same f.c.c. structure in

the actinide sublattice. Therefore, similar structure of exchange interactions could be expected.

UO_2 has been studied most intensively and now is much better understood in comparison with PuO_2 and UN. UO_2 is experimentally known to have a transverse 3-k magnetic structure and oxygen sub-lattice distortion of the same symmetry.¹¹ To the best of our knowledge, the only first-principles modelling of the non-collinear magnetic ordering in UO_2 was published by Laskowski *et al.*¹² This study employed the DFT + U technique within the local spin density approximation (LSDA)¹³ and all-electron linearized augmented plane wave plus local orbitals method (L/APW + lo)¹⁴ as implemented in the Wien2k computer code. In these computations, the energetic preference of the 3-k structure with respect to a regular 1-k structure was primarily dependent on the method used to correct for a double counting of on-site interactions. The 3-k structure appears to be more stable, if the double counting correction accurately includes spin-polarization of the electron density,¹² like it is done in LSDA + U ^{15,16} or in a simplified rotationally-invariant approach by Dudarev *et al.*¹⁷ Nevertheless, the 1-k and 2-k magnetic structures^{2,18} were also suggested for UO_2 prior to ref. 11. Also, no significant lattice distortions were found in these early experimental studies of UO_2 . Only recently, it was shown computationally¹⁹ for collinear AFM ordering in UO_2 that the U magnetic moments alternate along the $\langle 111 \rangle$ direction, but not along the $\langle 001 \rangle$ direction, as it was generally assumed in nearly all previous computer simulations. For simplicity, we call these structures hereafter as the “ $\langle 111 \rangle$ magnetic structure” and the “ $\langle 001 \rangle$ magnetic structure”. The study¹⁹ based on the electronic structure calculations with hybrid exchange–correlation functional found that the rhombohedral unit cell has a lower energy than the tetragonal one, even though the SOI are not included. Thus, change from usual $\langle 001 \rangle$ magnetic structure to the $\langle 111 \rangle$ one could indicate possible non-collinear magnetism.

To the best of our knowledge, no such studies on the magnetic properties of PuO_2 and UN have been performed so far. The X-ray diffraction measurements on UN revealed no significant tetragonal distortion,²⁰ which would be a consequence of the AFM spin alignment along the $\langle 001 \rangle$ direction.

^a European Commission, Joint Research Centre, Institute for Transuranium Elements, Postfach 2340, Karlsruhe, D-76125, Germany. E-mail: EHeif5719@sbcglobal.net

^b Institute for Solid State Physics, University of Latvia, Kengaraga 8, LV-1063, Riga, Latvia. E-mail: gryaznov@mail.com

^c Institute of Chemical Technology, Technicka 5, 16628 Prague, Czech Republic. E-mail: David.Sedmidubsky@vscht.cz

In the present study, we consider possible collinear and non-collinear magnetic structures of UO_2 also using the DFT + U technique, but implemented in another code, Vienna Ab initio Simulation Package (VASP).^{21,22} First, we test the ability of this method and the code to reproduce experimentally observed non-collinear magnetic order in UO_2 using experimental values of the Hubbard parameter ($U = 4.6$ eV, $J = 0.5$ eV).²⁴ Second, we explore different possible magnetic structures in UN and PuO_2 using the same DFT + U technique and try to determine which of the $\langle 001 \rangle$ and $\langle 111 \rangle$ structures is more stable. Section 2 describes computational details used in the present simulations. Descriptions of studied magnetic structures are given in Section 3. The results of our computations are provided and discussed in Section 4. Lastly, the conclusions are summarized in Section 5.

2. Computational details

In the present first-principles simulations we used the VASP (version 4.6)^{21,22} computer code employing the DFT + U method. The VASP code treats core electrons using pseudopotentials, whereas the semi-core electrons at U atoms and all the valence electrons are represented by plane waves. The electronic structure is calculated within the projector augmented wave (PAW) method.²³ The simplified rotationally-invariant Dudarev's form¹⁷ for the Hubbard correction was used for UO_2 and UN. It uses exclusively the difference, $U_{\text{eff}} = U - J$, of the Hubbard parameter U and the exchange parameter J . In contrast to uranium compounds, PuO_2 shows a significant role of exchange part requiring the use of Liechtenstein's form¹⁶ for the energy correction. The double counting correction in all our calculations was treated with account for spin-polarization.^{15–17} Computations of UO_2 were done including the SOI effects, whereas computations of PuO_2 and UN employed only scalar relativistic approximation. Both unit cell parameters and atomic positions were optimized until the energy convergence reached 10^{-5} eV. The calculations were performed with the cut-off energy of 520 eV. The integrations in the reciprocal space over the Brillouin zone (BZ) of the tetragonal unit cell of PuO_2 and UN (used to calculate the $\langle 001 \rangle$ AFM magnetic structure) were performed using $10 \times 10 \times 8$ and $12 \times 12 \times 10$ Monkhorst–Pack meshes,²⁵ respectively. Computations of the rhombohedral PuO_2 and UN with the $\langle 111 \rangle$ magnetic structure were performed with $12 \times 12 \times 12$ and $14 \times 14 \times 14$ Monkhorst–Pack meshes. Similarly, the integrations over the BZ for the conventional unit cell of UO_2 were performed using $6 \times 6 \times 6$ Monkhorst–Pack meshes. The conventional 12-atom unit cell was necessary for modelling of UO_2 with non-collinear magnetic structures. It was possible to use the smaller unit cell for a collinear magnetic ordering (the 1-k AFM $\langle 001 \rangle$ and $\langle 111 \rangle$ magnetic structures) in UO_2 . Correspondingly, in these cases we applied larger $14 \times 14 \times 10$ and $12 \times 12 \times 12$ k-meshes. The applied meshes in the reciprocal space were sufficient to reach a convergence of 10^{-4} eV for one-electron energies. Fractional electron occupancies were estimated with the Gaussian method using the smearing parameter of 0.25 eV. Calculations, which included SOI, were done with lifted symmetry constraints.

Photoemission spectroscopy (PS) measurements by Baer and Schoenes²⁴ suggest that the Hubbard correlation parameter U is 4.6 eV for UO_2 assuming that exchange parameter J is 0.5 eV. These values were applied later by Dudarev *et al.*¹⁷ In their calculations¹⁷ the band gap becomes open and equal to 1.3 eV within the LSDA + U , being, however, smaller than the experimental value of 2.0 eV. A somewhat better agreement is observed within the generalized gradient approximation,²⁶ *i.e.* GGA + U .^{10,27–29} Note that following Dudarev's calculations, we employed recently the same values of U and J in our study on bulk properties and defects behaviour in UO_2 .¹⁰ In the present simulations we used the same set of correlation U and exchange J parameters for computations of UO_2 . The parameter $U_{\text{eff}} = 1.875$ eV for UN was fitted³⁰ to reproduce the magnetic moment of uranium ions and UN unit cell volume in the low-temperature phase. The band gap of ~ 1.8 eV³¹ for PuO_2 is known from the electrical conductivity measurements which is similar to the band gap in UO_2 . Previous theoretical studies^{6–9} also agreed on the AFM solution for PuO_2 within the 1-k magnetism and, therefore, used the tetragonal structure as described above. Despite the relatively similar band gaps in both oxides, their electronic structures are quite different which is clearly seen in the corresponding PS measurements.³² Parameters $U = 3.0$ eV and $J = 1.5$ eV were fitted for PuO_2 to describe correctly its experimental lattice constant, band gap, and position of Pu 5f band.

3. Magnetic structures

The dependence of atomic magnetic moments on the position in a lattice can be expressed as expansion in plane waves:

$$\mathbf{M}_j = \sum_{w=1}^k e^{i\mathbf{k}_w(\mathbf{r}_j - \mathbf{r}_0)} \mathbf{M}_0^w,$$

where \mathbf{M}_j is the magnetic moment of the atom in unit cell j and at position \mathbf{r}_j , \mathbf{r}_0 is the position of the same atom in the 0th unit cell, \mathbf{k}_w and \mathbf{M}_0^w are, respectively, the wave vector and amplitude of the magnetic wave w .

In the collinear 1-k magnetic structures magnetic moments of U atoms are collinear and changes in the magnetic moments can be described by a single wave ($k = 1$). For the $\langle 001 \rangle$ magnetic structure choosing the Oz axis along the direction of alternation of magnetic moments, the wave vector is $\mathbf{k}_1 = 2\pi/a(0, 0, 1)$, where a is a cubic lattice constant. Similarly, for the $\langle 111 \rangle$ structure the wave vector is $\mathbf{k}_1 = \pi/a(1, 1, 1)$. These two collinear 1-k magnetic structures were modelled for all three materials considered here. These magnetic structures have symmetry reduced from the cubic one. In the $\langle 001 \rangle$ structure the lattice has a tetragonal symmetry, and in the $\langle 111 \rangle$ structure the lattice becomes rhombohedral, as can be seen from the next section.

Farber *et al.*¹⁸ suggested the 2-k transverse magnetic structure for UO_2 which is associated with a transverse phonon. If we choose the direction of the phonon propagation as the Oy axis, then magnetic waves propagate along the Ox and Oz axes ($\mathbf{k}_1 = 2\pi/a(1, 0, 0)$, $\mathbf{k}_2 = 2\pi/a(0, 0, 1)$) with amplitudes $\mathbf{M}_0^1 = M_0(0, 1, 0)$, $\mathbf{M}_0^2 = M_0(1, 0, 0)$, where M_0 is

the magnitude of atomic magnetic moment. Magnetic moments of U atoms lie on the Oxy plane and point along various $[110]$ directions. The transverse phonon in this structure can be described as O atoms in odd and even $\{010\}$ oxygen planes shift in opposite directions along the Ox axis. While later experiments showed that this structure is not the most stable one, we included it into our simulations to compare energies of all previously considered magnetic structures of UO_2 .

According to the experiment,¹¹ UO_2 has transverse 3-k magnetic structure. The wave vectors for three waves in 3-k structures are $\mathbf{k}_1 = 2\pi/a (1, 0, 0)$, $\mathbf{k}_2 = 2\pi/a (0, 1, 0)$, and $\mathbf{k}_3 = 2\pi/a (0, 0, 1)$. There are two equivalent transverse structures with this symmetry in the fluorite lattice. The first structure has amplitudes $\mathbf{M}_0^1 = M_0 (0, 1, 0)$, $\mathbf{M}_0^2 = M_0 (0, 0, 1)$, $\mathbf{M}_0^3 = M_0 (1, 0, 0)$. The second one has amplitudes $\mathbf{M}_0^1 = M_0 (0, 0, 1)$, $\mathbf{M}_0^2 = M_0 (1, 0, 0)$, $\mathbf{M}_0^3 = M_0 (0, 1, 0)$. The two O atoms nearest to each U atom in the direction of its magnetic moment shift from their sites toward this U atom. Both structures have the same total energies. We used the first one in our simulations.

4. Results and discussion

In the present study, we assess the difference between the two $\langle 111 \rangle$ and $\langle 001 \rangle$ AFM magnetic collinear structures, as a function of the U and J parameters for UN and PuO_2 (Fig. 1).

The energy difference between the two magnetic structures for UN (Fig. 1a) is very small and negative at small values of $U_{\text{eff}} = U - J$. It slowly grows for U_{eff} between 0.0 eV and 1.5 eV, then noticeably increases from 2.0 to 5 eV, and likely saturates for the higher values of U_{eff} . For the optimized value of $U_{\text{eff}} = 1.875$ eV the $\langle 001 \rangle$ structure of UN is already more stable than the $\langle 111 \rangle$ structure (see inset in Fig. 1a). At this value of U_{eff} the lattice constants for UN in the $\langle 001 \rangle$ magnetic structure are $a = 4.974$ Å and $c = 4.859$ Å, and lattice parameters in the $\langle 111 \rangle$ magnetic structure are the lattice constant $a = 4.942$ Å and the rhombohedral angle $\gamma = 88.2^\circ$. In both cases the cubic unit cell is distorted along the direction of alternation of magnetic moments. In the $\langle 001 \rangle$ structure it is compressed along the Oz axis, for the $\langle 111 \rangle$ structure the unit cell is elongated along $[111]$ direction. It is experimentally known that UN is cubic with the lattice constant $a = 4.886$ Å.³³ The calculated spin magnetic moments of U atoms are $1.47 \mu_B$ in the $\langle 001 \rangle$ structure and $1.82 \mu_B$ in the $\langle 111 \rangle$ structure. The magnetic moment of U atoms measured¹ at low temperatures is $0.75 \mu_B$. Inclusion of the SOI allows revealing substantial orbital moments in actinide compounds which would lead to much better alignment of U atom magnetic moment with experimental value.³⁰ It is important also that the value of $U_{\text{eff}} = 1.875$ eV is sufficient to stabilize the AFM structure with respect to the FM one in contrast to standard DFT calculations.^{30,34}

Due to the Liechtenstein form of the DFT + U functional¹⁶ applied to PuO_2 , we have to vary the U - and J -parameters independently. It was done by varying U - with the J -parameter fixed at 1.5 eV and by varying J at $U = 3.0$ eV, correspondingly. As seen in Fig. 1b, the $\langle 001 \rangle$ magnetic structure of PuO_2 is energetically more stable than the $\langle 111 \rangle$ one, except

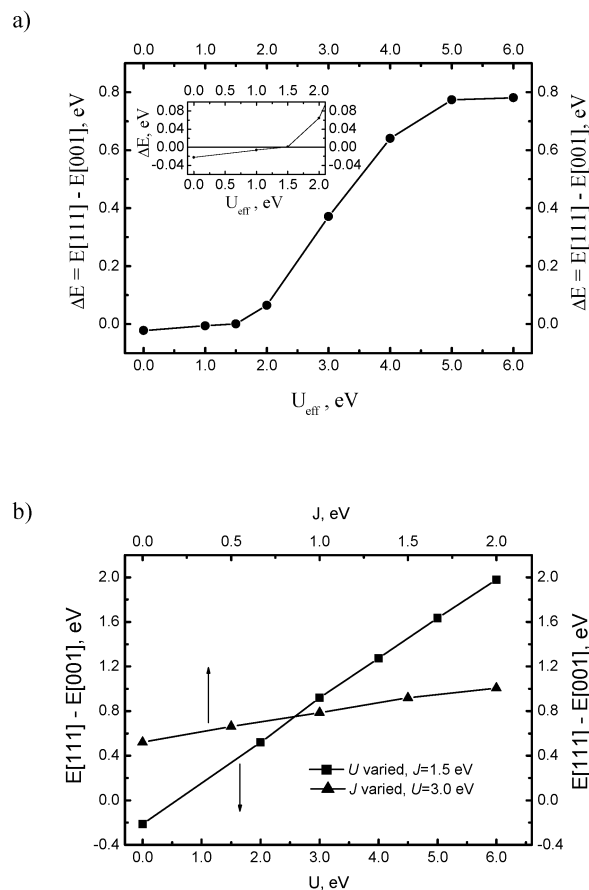


Fig. 1 The energy difference between the $\langle 111 \rangle$ and $\langle 001 \rangle$ magnetic structures for (a) UN as a function of U_{eff} (Dudarev's functional); the inset contains enlarged fragment of the same plot at $U_{\text{eff}} \leq 2.0$ eV; (b) PuO_2 as functions of one of the U and J parameters (Lichtenstein's functional), while another parameter is fixed.

for very small values of Hubbard parameter U . It suggests no preference of the $\langle 111 \rangle$ magnetic structure, in contrast to UO_2 (see discussion below), for realistic values of U - and J -parameters. The difference increases with both parameters, indicating further stabilization of the $\langle 001 \rangle$ magnetic structure in a comparison to the $\langle 111 \rangle$ one. The energy difference between the two magnetic structures (Fig. 1b) is almost linear for PuO_2 , independently of which parameter is varied or fixed. For chosen values of the parameters ($U = 3.0$ eV and $J = 1.5$ eV), lattice constants for PuO_2 in the $\langle 001 \rangle$ structure are $a = 5.402$ Å and $c = 5.513$ Å, and lattice parameters in the $\langle 111 \rangle$ magnetic structure are $a = 5.430$ Å and $\gamma = 88.9^\circ$. In the case of PuO_2 a cubic unit cell becomes elongated in the direction of alternation of magnetic moments. The calculated spin magnetic moments of Pu atoms are $3.81 \mu_B$. Experimentally, PuO_2 is cubic with lattice constant $a = 5.398$ Å³⁵ and diamagnetic.⁵

In Fig. 2 we present the total densities of states (DOS) for the discussed tetragonal AFM unit cell of PuO_2 , when the strong correlation effects are neglected (dashed line) and for the employed values of $U = 3.0$ eV and $J = 1.5$ eV (solid line). The DOS clearly demonstrates that PuO_2 , like UO_2 , tends to be metallic if the strong correlation effects are not treated

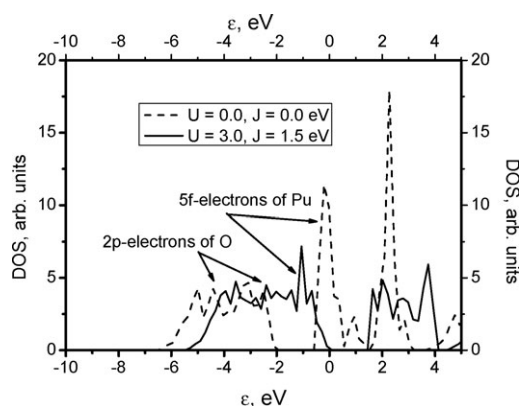


Fig. 2 A comparison of total density states (DOS) for PuO_2 for $U = 0.0, J = 0.0$ eV (dashed line) and $U = 3.0, J = 1.5$ eV (solid line). The DOS was calculated by employing the tetrahedron method²⁹ with given occupations of the electron states. The Fermi energy is taken as zero; ε is one-electron energy.

properly, whereas the band gap of 1.5 eV appears for the chosen parameters of the GGA + U scheme. The latter value of the band gap is slightly smaller than the experimental value (1.8 eV).

The case of UO_2 differs from the discussed above trends for UN and PuO_2 , reflecting the fact that the $\langle 111 \rangle$ magnetic structure in UO_2 is more stable than the $\langle 001 \rangle$ one by 62 meV per formula unit at $U = 4.6$ eV and $J = 0.5$ eV. This result confirms the previously published hybrid functional calculations¹⁹ with atomic basis set. Due to the SOI the total energy is reduced almost by 2.66 eV per UO_2 primitive unit cell. This does not affect relative energies of all studied magnetic structures (3-k, 2-k and both $\langle 001 \rangle$ and $\langle 111 \rangle$ 1-k structures). Relative energies for all considered magnetic structures are provided in Table 1 with respect to the 3-k magnetic structure. The transverse 3-k magnetic structure appears to be the most energetically preferable. This is in accord with inelastic neutron scattering experiments.¹¹ The 2-k structure proposed by Faber and Lander¹⁸ has just a little bit lower energy (5 meV per formula unit) than the $\langle 111 \rangle$ collinear structure but noticeably higher than the transverse 3-k structure.

Both the $\langle 001 \rangle$ and $\langle 111 \rangle$ collinear structures have unit cells compressed along the direction of alternation of magnetic moment (see Table 1). Magnetic moments of U atoms in both structures point in the same $[001]$ and $[111]$ directions.

Table 1 Results of calculations for UO_2 . ΔE is the total energy (in meV per molecule) for various magnetic structures in UO_2 with respect to transverse 3-k structure, which has the lowest energy. The energy calculations included SOI. a, b and c are lattice constants, α, β and γ are angles between lattice vectors of conventional unit cell. E_g is band gap. μ is the total magnetic moment of U atom (in Bohr's magnetons μ_B) and the values in parentheses are spin contributions to the magnetic moments. The experimental value of magnetic moment is 1.74 μ_B

	Magnetic structure			
	$\langle 001 \rangle$ 1-k	$\langle 111 \rangle$ 1-k	Faber–Lander 2-k	Transverse 3-k
$\Delta E/\text{meV}$ per molecule	95	33	28	0
$a/\text{\AA}$	5.566	5.550	5.555	5.547
$b/\text{\AA}$	5.566	5.550	5.562	5.547
$c/\text{\AA}$	5.508	5.550	5.521	5.547
$\alpha = \beta = \gamma/^\circ$	90	91.7	90	90
E_g/eV	1.95	2.03	2.50	2.38
μ/μ_B	1.76 (1.95)	2.00 (1.98)	1.81 (2.04)	1.99 (2.00)

All lattice constants in the 2-k structure are different. The lattice of the 2-k structure becomes orthorhombic. As expected (see Section 3 and ref. 18), odd and even oxygen $\{010\}$ planes are shifted along the O_x axis in the opposite directions. The obtained shift is $\Delta = 9.7 \times 10^{-3}a$ (compare with $\Delta = 2.6 \times 10^{-3}a$ obtained in ref. 10). However, directions of magnetic moments are very different from those suggested in ref. 11: the magnetic moments point almost along the $[010]$ directions, but are slightly tilted towards shorter square diagonal (the squares are perpendicular to the $[001]$ direction). This can be expressed by amplitudes of magnetic waves $M_0^1 = (0, 1, 0)1.79 \mu_B$, $M_0^2 = (1, 0, 0)0.24 \mu_B$.

Unit cell in the transverse 3-k structure keeps cubic shape. Magnetic moments are aligned according to the transverse 3-k symmetry. The pair of O atoms nearest to each U atom in the direction of its magnetic moment is shifted toward this U atom by $9.6 \times 10^{-3}\sqrt{3}a$ (or 0.092 \AA). Somewhat smaller distortion was derived from experiments.¹⁸

For the total magnetic moments of U atoms in the most stable transverse 3-k structure we obtained a value of 1.99 μ_B , which slightly exceeds the experimental value of 1.74 μ_B . Magnetic moments obtained for the $\langle 001 \rangle$ 1-k and for the 2-k structures are much closer to the experimental value, but these structures have higher energies and are not consistent with inelastic neutron scattering data.¹¹ According to Ippolito *et al.*³⁶ the magnetic moment reduction can be explained by a dynamic Jahn–Teller mixing, while our modelling includes only a static Jahn–Teller mixing. The obtained values of magnetic moments are still noticeably lower than the magnetic moment of 2.06 μ_B of U ions in the ground state expected from the intermediate coupling of moments.³⁵ We have to notice that the intermediate coupling theory includes a multi-determinant form of wavefunction, while the present simulations are done in a single-determinant form of wavefunction.

In Fig. 3 we compare the total DOS for different magnetic UO_2 structures. In all considered structures, the highest valence band consists predominantly of U 5f orbitals and the next highest valence band is mostly built from O 2p orbitals. The conduction bands contain U 6d and U 5f orbitals. Our calculations reproduce the band gaps in various magnetic structures of UO_2 (see Table 1) very close to the experimental value (2.0 eV).²⁴ The band gaps in both considered non-collinear structures are a little larger, by several tenths of eV. In calculations¹⁹ with hybrid

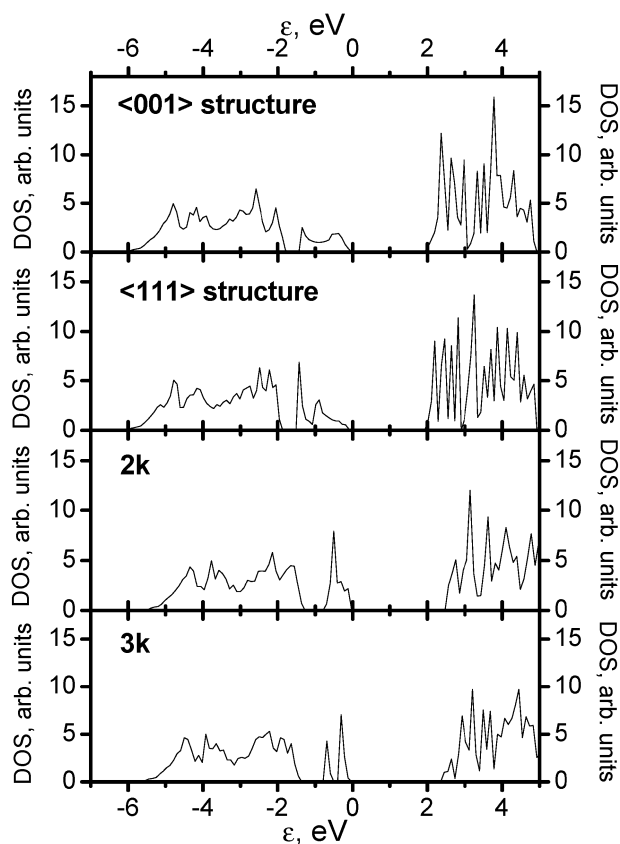


Fig. 3 The total DOS of UO_2 calculated for $\langle 001 \rangle$, $\langle 111 \rangle$, 2-k and 3-k structures. The Fermi energy is taken as zero; ϵ is one-electron energy.

functional the band gap for the $\langle 111 \rangle$ structure is significantly (by ~ 1.5 eV) overestimated.

The U 5f band width is 1.5 eV for the collinear magnetic structures and gets much narrower for the non-collinear cases (0.76 eV and 0.86 eV in case of 2-k and 3-k structures, respectively). This band splits into two separate sub-bands: U 5f(5/2) and U 5f(7/2) in the 3-k structure with a gap of ~ 0.1 eV and distance between peaks ~ 0.38 eV. The width (~ 4.2 eV for $\langle 111 \rangle$ structure and ~ 4.4 eV for other structures) of O 2p band varies little among considered structures. The gap between O 2p and U 5f valence bands is small, ~ 0.3 – 0.5 eV. As a result, O 2p band shifts, following the narrowing of U 5f valence band, and becomes by ~ 0.5 eV closer to the Fermi level in the non-collinear structures than in the collinear ones.

5. Conclusions

We have compared several possible magnetic structures of several key actinides UO_2 , UN and PuO_2 based on the GGA + U technique. Our modelling shows that the transverse non-collinear 3-k structure of UO_2 is the most stable one for this material. UO_2 retains a cubic shape in this structure. Two O atoms nearest to each U atom in the direction of its magnetic moment move toward this U atom. This is consistent with both experiment¹¹ and previous computer simulation¹² employing the LDA + U technique within the Wien2k code. It is important that such agreement is achieved with the standard

values of Hubbard and exchange parameters ($U = 4.6$ eV, $J = 0.5$ eV) within Dudarev's form of the DFT + U approach.¹⁷ Still, a reason for overestimated U atom magnetic moment remains unclear.

The collinear magnetic order causes breaking of cubic symmetry in UN and PuO_2 . In contrast to UO_2 , neither UN nor PuO_2 show the energetical preference for the rhombohedral distortion. Both materials have the AFM tetragonal $\langle 001 \rangle$ structure for a reasonable choice of parameters U and J . The total DOS of PuO_2 is successfully reproduced using the Liechtenstein form¹⁶ for the Hubbard correction with the parameters $U = 3.0$ eV and $J = 1.5$ eV. However, as well as in the previous computational studies,^{6–9} we obtained that the AFM state of PuO_2 is more stable than the experimentally observed diamagnetic state.⁵

Acknowledgements

This study was supported by the F-BRIDGE project, as part of the 7th EC Framework Programme, and the Proposal Nr. 25592 from the EMS Laboratory of the PNNL. Authors are greatly indebted to E. Kotomin, R. Caciuffo, G. Lander, R. A. Evarestov, R. Konings for very useful discussions. We acknowledge also the EC for support in the frame of the Program "Training and mobility of researchers".

Notes and references

- 1 N. A. Curry, *Proc. Phys. Soc.*, 1965, **86**, 1193.
- 2 B. C. Frazer, G. Shirane and D. E. Cox, *Phys. Rev.*, 1965, **140**(4a), A1448.
- 3 M. Marutzky, U. Barkow, J. Schoenes and R. Troć, *J. Magn. Mater.*, 2006, **299**, 225.
- 4 I. D. Prodan, G. E. Scuseria and R. L. Martin, *Phys. Rev. B: Condens. Matter Mater. Phys.*, 2007, **76**, 033101.
- 5 M. Colarieti-Tosti, O. Eriksson, L. Nordström, J. Wills and M. S. Brooks, *Phys. Rev. B: Condens. Matter Mater. Phys.*, 2002, **65**, 195102.
- 6 I. D. Prodan, G. E. Scuseria, J. A. Sordo, K. N. Kudin and R. L. Martin, *J. Chem. Phys.*, 2005, **123**, 014703.
- 7 G. Jomard, B. Amadon, F. Bottin and M. Torrent, *Phys. Rev. B: Condens. Matter Mater. Phys.*, 2008, **78**, 075125.
- 8 B. Sun, P. Zhang and X.-G. Zhao, *J. Chem. Phys.*, 2008, **128**, 084705.
- 9 F. Jollet, G. Jomard, B. Amadon, J. P. Crocombette and D. Torumba, *Phys. Rev. B: Condens. Matter Mater. Phys.*, 2009, **80**, 235109.
- 10 D. Gryaznov, E. Heifets and E. Kotomin, *Phys. Chem. Chem. Phys.*, 2009, **11**, 7241.
- 11 R. Caciuffo, G. Amoretti, P. Santini, G. H. Lander, J. Kulda and P. de V. Du Plessis, *Phys. Rev. B: Condens. Matter Mater. Phys.*, 1999, **59**, 13892.
- 12 R. Laskowski, G. K. H. Madsen, P. Blaha and K. Schwarz, *Phys. Rev. B: Condens. Matter Mater. Phys.*, 2004, **69**, 140408.
- 13 W. Kohn and L. J. Sham, *Phys. Rev.*, 1965, **140**, A1133.
- 14 P. Blaha, K. Schwarz, G. K. H. Madsen, D. Kvasnicka and J. Luitz, WIEN2k, *An Augmented Plane Wave + Local Orbitals Program for Calculating Crystal Properties*, ed. K. Schwarz, Techn. Universität Wien, Austria, ISBN 3-9501031-1-2, 2001.
- 15 M. T. Czyżyk and G. A. Sawatzky, *Phys. Rev. B: Condens. Matter*, 1994, **49**(20), 14211. The technique, proposed in this paper, is often called "around mean field" method. Under this name it is used in Wien2k code¹⁴ and in ref. 12.
- 16 A. I. Liechtenstein, V. I. Anisimov and J. Zaane, *Phys. Rev. B: Condens. Matter*, 1995, **52**, R5467.
- 17 S. L. Dudarev, G. A. Botton, S. Y. Savrasov, C. J. Humphreys and A. P. Sutton, *Phys. Rev. B: Condens. Matter Mater. Phys.*, 1998, **57**(3), 1505.

- 18 J. Faber, Jr and G. H. Lander, *Phys. Rev. B: Solid State*, 1976, **14**(3), 1151; J. Faber, Jr, G. H. Lander and B. R. Cooper, *Phys. Rev. Lett.*, 1975, **35**, 1770.
- 19 R. A. Evarestov, A. Bandura and E. Blokhin, *Acta Mater.*, 2009, **57**, 600.
- 20 H. W. Knott, G. H. Lander, M. H. Mueller and O. Vogt, *Phys. Rev. B: Condens. Matter*, 1980, **21**(9), 4159.
- 21 G. Kresse and J. Furthmüller, *Comput. Mater. Sci.*, 1996, **6**, 15.
- 22 G. Kresse and J. Furthmüller, *VASP, the Guide*, University of Vienna, 2007.
- 23 G. Kresse and D. Joubert, *Phys. Rev. B: Condens. Matter Mater. Phys.*, 1999, **59**(3), 1758.
- 24 Y. Baer and J. Schoenes, *Solid State Commun.*, 1980, **33**, 885.
- 25 J. Monkhorst and J. D. Pack, *Phys. Rev. B: Solid State*, 1976, **13**, 5188.
- 26 J. P. Perdew, K. Burke and M. Ernzerhof, *Phys. Rev. Lett.*, 1996, **77**, 3865.
- 27 H. Y. Geng, Y. Chen, Y. Kaneda and M. Kinoshita, *Phys. Rev. B: Condens. Matter Mater. Phys.*, 2007, **75**, 054111.
- 28 M. Iwasawa, Y. Chen, Y. Kaneta, T. Ohnuma, H.-Y. Geng and M. Kinoshita, *Mater. Trans.*, 2006, **47**(11), 2651.
- 29 F. Gupta, G. Brillant and A. Pasturel, *Philos. Mag.*, 2007, **87**, 2561.
- 30 D. Gryaznov, E. Heifets, E. A. Kotomin, in preparation.
- 31 C. E. McNeilly, *J. Nucl. Mater.*, 1964, **11**(1), 53.
- 32 T. Gouder, A. Seibert, L. Havela and J. Rebizant, *Surf. Sci.*, 2007, **601**, L77.
- 33 H. Matzke, *Science of Advanced LMFBR Fuels*, North Holland, Amsterdam, 1986.
- 34 R. Atta-Fynn and A. K. Ray, *Phys. Rev. B: Condens. Matter Mater. Phys.*, 2007, **76**, 115101.
- 35 J. M. Haschke, T. H. Allen and L. A. Morales, *Science*, 2000, **287**, 285.
- 36 D. Ippolito, L. Martinelli and G. Bevilacqua, *Phys. Rev. B: Condens. Matter Mater. Phys.*, 2005, **71**, 064419.